Generation of Solution and Surface Gradients Using Microfluidic Systems

Noo Li Jeon, Stephan K. W. Dertinger, Daniel T. Chiu, Insung S. Choi, Abraham D. Stroock, and George M. Whitesides*

Department of Chemistry and Chemical Biology, Harvard University, Cambridge, Massachusetts 02138

Received April 24, 2000. In Final Form: July 13, 2000

This paper describes a simple, versatile method of generating gradients in composition in solution or on surfaces using microfluidic systems. This method is based on controlled diffusive mixing of species in solutions that are flowing laminarly, at low Reynolds number, inside a network of microchannels. We demonstrate the use of this procedure to generate (1) gradients in the compositions of solutions, measured directly by colorimetric assays and (2) gradients in topography of the surfaces produced by generating concentration gradients of etching reagents, and then using these gradients to etch profiles into the substrate. The lateral dimensions of the gradients examined here, which went from 350 to 900 μm, are determined by the width of the microchannels. Gradients of different size, resolution, and shape have been generated using this method. The shape of the gradients can be changed continuously (dynamic gradients) by varying the relative flow velocities of the input streams of fluids. The method is experimentally simple and highly adaptable, and requires no special equipment except for an elastomeric relief structure that can be readily prepared by rapid prototyping. This technique provides a new platform with which to study phenomena that depend on gradients in concentration, especially dynamic phenomena in cell biology (chemotaxis and haptotaxis) and surface chemistry (nucleation and growth of crystals, etching, and Marangoni effects).

Introduction

Gradients in the properties of surfaces and solutions are important in many processes, both biological (chemotaxis[1−6] and nerve growth cone guidance[7,8]) and chemical (nucleation and growth of crystals).[9−11] Creating well-defined gradients in surface and solution properties to study chemotaxis on scales relevant to chemistry and biology—dimensions of a few microns to a few hundred microns—has been a substantial experimental challenge.[5] Cell biology poses particular challenges; because chemotactic cells are sensitive to concentration differences as low as 2% between the front and back of the cell,[2] gradients with resolutions on the order of a single cell (10−100 μm) are required, that is, 2−20% per 100 μm. Present methods for generating gradients in solution using a pipet tip or a reservoir in a gel cannot provide the required spatial control.[3,5,11] These methods also have limitations in the shape of gradients that can be created, because they rely on simple diffusion of the chemical species between a "source" and a "sink".[3,5,11] The spatial resolution that can be achieved with these conventional techniques typically is on the order of several millimeters.

A number of methods have been demonstrated previously that use self-assembled monolayers (SAMs) to generate gradients in surface properties; these include cross diffusion,[12,13] photoimmobilization of peptides on SAMs,[14,15] and electrochemical desorption.[16] These techniques are limited in the kinds of chemistry that they can incorporate; it is also difficult to use them to produce gradients with sizes on the order of biological cells (10−100 μm).

The ability to generate gradients of proteins, surface properties, and fluid streams containing growth factors, toxins, enzymes, drugs, and other types of biologically relevant molecules by simple experimental procedures will offer a broadly useful capability in biology and chemistry. This paper describes a simple, versatile method of generating gradients in compositions of solutions or surfaces using microfluidics and gives examples of static and dynamic gradients. We have focused our initial studies on two types of gradients: (1) gradients in the composition of solution, measured directly by colorimetric assays and (2) gradients in topography of the surface, produced by generating concentration gradients of etching reagents and then using these gradients to etch profiles into the substrate.

Experimental Section

Fabrication of the Gradient Generator. The microfluidic gradient generator was fabricated in poly(dimethylsiloxane) (PDMS) using rapid prototyping[17,18] and soft lithography.[19]

* Corresponding author. E-mail: gwhitesides@gmwgroup.harvard.edu. Fax: (617) 495-9857. Tel: (617) 495-9430.

(1) Dekker, L. V.; Segal, A. W. *Science* **2000**, *287*, 982−985.
(2) Parent, C. A.; Devreotes, P. N. *Science* **1999**, *284*, 765−770.
(3) Weiner, O. D.; Servant, G.; Welch, N. D.; Mitchison, T. J.; Sedat, J. W.; Bourne, H. R. *Nature Cell Biol.* **1999**, *1*, 75−81.
(4) Zicha, D.; Dunn, G. A.; Jones, G. E. *Analysing Chemotaxis Using the Dunn Direct-Viewing Chamber*; Pollard, J. W., Ed., 1997; Vol. 75, pp 449−458.
(5) Wilkinson, P. C. *J. Immun. Methods* **1998**, *216*, 139−153.
(6) Grebe, T. W.; Stock, J. *Curr. Biol.* **1998**, *8*, R154−R157.
(7) Song, H. J.; Poo, M. M. *Curr. Opin. Neurobiol.* **1999**, *9*, 355−363.
(8) Zheng, J. Q.; Poo, M. M.; Connor, J. A. *Perspect. Dev. Neurobiol.* **1996**, *4*, 205−213.
(9) Aizenberg, J.; Black, A. J.; Whitesides, G. M. *Nature* **1999**, *398*, 495−498.
(10) Aizenberg, J.; Black, A. J.; Whitesides, G. M. *J. Am. Chem. Soc.* **1999**, *121*, 4500−4509.
(11) Gallardo, B. S.; Gupta, V. K.; Eagerton, F. D.; Jong, L. I.; Craig, V. S.; Shah, R. R.; Abbott, N. L. *Science* **1999**, *283*, 57−60.
(12) Liedberg, B.; Tengvall, P. *Langmuir* **1995**, *11*, 3821−3827.
(13) Liedberg, B.; Wirde, M.; Tao, Y. T.; Tengvall, P.; Gelius, U. *Langmuir* **1997**, *13*, 5329−5344.
(14) Herber, C. B.; McLernon, T. L.; Hypolite, C. L.; Adams, D. N.; Pikus, L.; Huang, C. C.; Fields, G. B.; Letourneau, P. C.; Distefano, M. D.; Hu, W. S. *Chem. Biol.* **1997**, *4*, 731−737.
(15) Hypolite, C. L.; McLernon, T. L.; Adams, D. N.; Chapman, K. E.; Herbert, C. B.; Huang, C. C.; Distefano, M. D.; Hu, W. S. *Bioconjug. Chem.* **1997**, *8*, 658−663.
(16) Terrill, R. H.; Balss, K. M. Z., Y.; Bohn, P. W. *J. Am. Chem. Soc.* **2000**, *122*, 988−989.

10.1021/la000600b CCC: $19.00
Published on Web 10/07/2000

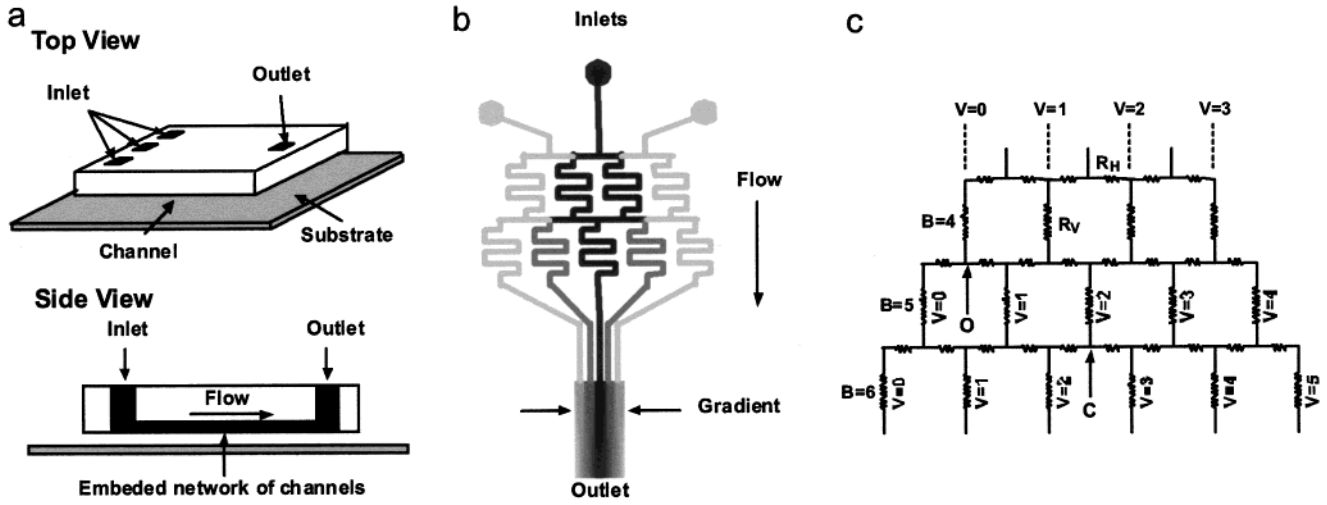

Figure 1. (a) Scheme of the PDMS microfluidic gradient generator used in this work. (b) Schematic design of a representative gradient-generating microfluidic network. Solutions containing different chemicals were introduced from the top inlets and allowed to flow through the network. The fluid streams were repeatedly combined, mixed, and split to yield distinct mixtures with distinct compositions in each of the branch channel. When all the branches were recombined, a concentration gradient was established across the outlet channel. The width of this channel and the total number of the branches determined the width of the gradient and the resolution of the steps making up the gradient, respectively. (c) Equivalent electronic circuit model of the pyramidal microfluidic network.

Briefly, a high-resolution printer was used to generate a mask (in the form of a transparency) from a CAD file. The transparency mask (which can have a minimum feature size of ~20 μm, when generated by a 3300 dpi printer) was used in 1:1 contact photolithography with SU-8 photoresist (MicroChem, Newton, MA) to generate a negative "master", consisting of patterned photoresist on a Si wafer. Positive replicas with embossed channels were fabricated by molding PDMS against the master, as described previously.[17−19] The PDMS replica was placed against a flat substrate (a glass slide or Si wafer) and held in place by van der Waals contact forces; this assembly produced the required systems of microfluidic channels.[18] Inlet and outlet ports (1 mm diameter holes) for the fluids were punched out of the PDMS using a sharpened needle. Polyethylene tubing with outer diameter slightly larger than the inner diameter of the port was inserted into the hole to make the fluidic connections. These connections were then sealed with epoxy glue (5 min Epoxy, Devcon, MA). The pieces of tubing were then connected to a syringe pump to complete the fluidic device.

Results and Discussion

Design of the Gradient Generator. Figure 1a shows a schematic of a typical PDMS device of the type we used throughout these studies for the generation of gradients. We used a network of microchannels having three inlets. Each inlet was connected to syringes that contained solutions of chemicals of different concentrations. We infused the three solutions simultaneously into the microfluidic network. As the fluid streams traveled down the network, they were repeatedly split, mixed, and recombined. After several generations of branched systems, each branch contained different proportions of the infused solutions. When all the branches were brought together into a single channel, a gradient was established across this channel, perpendicular to the flow direction. Figure 1b shows the basic design of the microfluidic network used in this prototype gradient generator.

To predict the profile of the concentration gradient at the outlet of this pyramidal microfluidic network, we have to understand the splitting ratio of flows at each branching point of this network. For convenience, we define the part of the network that contains n vertical channels as being an nth order branched system **($B = n$).** In addition, we label each vertical channel **(V)**, within each branched system, from left to right as $V = 0$, $V = 1$, and $V = B - 1$ (see Figure 1c).

The analysis of the splitting of fluid flow can be understood by making an analogy with an equivalent electronic circuit (Figure 1c). In this analysis, we make the approximation that the resistance of the horizontal channels (R_H) is negligible in comparison with the resistance of vertical channels (R_V), $R_H \ll R_V$. This approximation is valid because the horizontal channels are much shorter (~20 times) than the vertical ones (the resistance to fluid flow scales linearly with the length of the channel in Poiseuille flow). Only the resistance of the vertical channels needs to be considered; here, we have maintained these resistances to be the same for all channels within each branch. In addition, the volume throughput in all vertical channels, within each branched system, is the same. In combination with the left−right symmetry of our microfluidic structure, we can derive the normalized splitting ratio at each branching point of our network: the amount of flow to the left is $[B - V]/[B + 1]$ and to the right is $[V + 1]/[B + 1]$. For example, at the branch point denoted O in Figure 1c ($B = 4$, $V = 0$), the relative volume of the flow to the left is 4/5 ($[4 - 0]/[4 + 1]$) and to the right is 1/5 ($[0 + 1]/[4 + 1]$), whereas at branch point C ($B = 5$, $V = 2$), the ratio of splitting is identical (1/2 to right and 1/2 to left), which reflects the left−right symmetry of our network design. With each additional branched system, therefore, the amount of fluid that flows from outer channels toward the ones at the center becomes progressively less; for the outermost channels, the ratio of flow toward the neighboring channels scales as $1/B$. This characteristic determines the shape of the concentration profiles when all the branch channels are brought together to a single channel at the end of the fluidic network.

The generation of gradients using a network of microfluidic channels is based on the controlled diffusive mixing of laminar flow fluids by repeated splitting, mixing, and

(17) Qin, D.; Xia, Y.; Whitesides, G. M. *Adv. Mater.* **1996**, *8*, 917−921.
(18) Duffy, D. C.; McDonald, J. C.; Schueller, O. J. A.; Whitesides, G. M. *Anal. Chem.* **1998**, *70*, 4974−4984.
(19) Xia, Y.; Whitesides, G. M. *Angew. Chem., Int. Ed. Engl.* **1998**, *37*, 550−575.

recombination of fluid streams. Under conditions of complete diffusive mixing of neighboring fluid streams in each vertical serpentine channel, the formula given above for calculating the splitting ratio can be used to predict the profile of the concentration gradient at the outlet of this microfluidic network. Since exchange of molecules between laminar streams occurs exclusively by diffusion, it is important that the interval of time that two laminar flow streams spend flowing side by side in the serpentine channel is sufficiently long that equilibration is complete: the length of the serpentine mixing zone was ~10 mm, and flow speeds were between 1 and 100 mm/s. The time required for complete equilibration can be estimated by solving the diffusion equation in one dimension in finite media taking into account the initial distribution for our particular case. An analytical solution for this problem is given by (eq 1)[20]

$$C(t,x) = \frac{1}{2}C_0 \sum_{n=-\infty}^{\infty}\left\{\text{erf}\frac{h + 2nl - x}{2\sqrt{Dt}} + \text{erf}\frac{h - 2nl + x}{2\sqrt{Dt}}\right\} \quad (1)$$

where $C(t,x)$ is the concentration at time t and at point x, D the diffusion coefficient in cm^2/s, t the time in s, l the width of the channel, h the width of the initial distribution, and C_0 the initial concentration in the channel. A numerical evaluation using the first 21 terms in the sum ($n = -10$ to $+10$, $D = 5 \times 10^{-6}$ cm^2/s, width 50 μm, width of initial distribution 25 μm) shows that 97% diffusive mixing is reached after 1 s. We define percent mixing across a channel of width l and at time t as

$$\%\ \text{mixing}(t) = \left(1 - \frac{\int_0^l |C(t) - C(\infty)|\ dx}{\int_0^l |C(0) - C(\infty)|\ dx}\right) \times 100\% \quad (2)$$

where $C(t)$, $C(\infty)$, and $C(0)$ are the concentration profiles across the width of the channel at times t, $t = \infty$, and $t = 0$, respectively.

Gradients in Solution. Figure 2a–c shows fluorescence micrographs of the concentration gradient of fluorescein isothiocynate (FITC) in aqueous solution with increasing flow speeds (1, 10, and 100 mm/s, respectively). The micrographs were taken from the top of the microfluidic network, looking through the PDMS. The white dotted lines identify the boundaries of the microfluidic channels not visible with fluorescence microscopy. The top portion of the photograph shows nine distinct branch channels (50 μm wide and 100 μm high) that are combined into a wider outlet channel (900 μm wide, 100 μm high). Each branch channel contained a distinct concentration of FITC solution.

A gradient generator similar in design to one described in Figure 1b was used for this experiment. The microchannels were formed by sealing the PDMS chip against a transparent glass slide. The gradient generator had three inlets. FITC (100 μM FITC in $NaHCO_3$ buffer, pH 8.3) was introduced at the center, and buffer (0% FITC) was introduced at the two outer inlets. The micrographs were taken while maintaining steady flow through the microfluidic network (fluid was injected at same speed into all three inlets). The graphs below the micrographs show the corresponding fluorescence intensity profile across the outlet channel at 500 μm downstream (dotted horizontal line) from the junction. The fluorescence intensity was normalized with respect to the starting solution (taking 100 μM FITC as 100%) and was expressed in terms of concentration. The round dots on the graph indicate the calculated concentration of each branch channel. These values were obtained by taking into account the inlet concentration of FITC and the flow splitting as discussed earlier.

Figure 2, a and b, shows FITC concentration gradient across the outlet channel for flow speeds of 1 and 10 mm/s. The maximum concentration of FITC was found at the center of the channel (57% in the center); the outer region of the outlet channel contained 0% FITC (that is, it is essentially pure buffer). The measured concentration profile of FITC across the outlet channel agreed well with the calculated value; this agreement indicates complete diffusive mixing of streams of fluids in the serpentine region of the fluidic channels. Considering that the length of each mixing zone (total length of the serpentine region) is 10 mm, at flow speeds of 1 and 10 mm/s, the resident time is 10 and 1 s, respectively. This result was expected, given that close to 97% mixing between fluid streams occur within 1 s as discussed earlier.

The difference in shapes of the intensity profiles—and in particular, the difference between the smooth gradient in 2a and the step gradient for 2b—is caused by differences in flow speeds. At a flow speed of 1 mm/s, considerable diffusive mixing (though not complete mixing) has occurred, and boundaries between the streams are blurred at the 500 μm point downstream from the junction. Figure 2b shows a step profile because at a flow speed of 10 mm/s, negligible diffusive mixing has occurred at this point (500 μm downstream); the rapid flow preserves the step profile of concentrations of the branch channels over substantial distances. When the flow speed was increased to 100 mm/s (Figure 2c), the micrograph shows distinct, sharp boundaries between streams, with a narrower profile than calculated, and with higher concentrations in the middle channels and lower concentrations in outer channels. This result was expected for a system with incomplete diffusive mixing in the serpentine regions of the mixing system. The evolution of the profile of the concentration gradient along the channel is governed by Fick's law of diffusion in one dimension (the direction perpendicular to the fluid flow): $\delta c/\delta t = D\ (\delta^2 c/\delta t^2)$.

Gradient in Topography. We have used several systems to check the performance of the gradient generator. In one, we generated a gradient in the concentration of HF, and used it to generate a gradient in topology in a thick SiO_2 layer (500 nm) on a Si wafer. Figure 3a shows the design of the microfluidic network used in this experiment. The serpentine channel design was chosen to give a mixing zone with the desired length (~10 mm) in a compact structure. The microfluidic channels are 50 μm wide and 100 μm high. To create the etched pattern shown in Figure 3b,c, a PDMS piece with embossed pattern of microchannels (Figure 3a) was brought into conformal contact with the Si/SiO_2 wafer. Three aqueous solutions containing water, HF (5% in water), and water were injected into inlets from left to right. The flow speeds of HF and water were kept at 1 mm/s. Where the HF solutions came into contact with the surface, they etched the SiO_2. Higher concentrations of HF etched SiO_2 more rapidly.

The reasons for choosing to etch a SiO_2/Si wafer as a measure of concentration and surface reactivity gradient were as follows: (1) the characteristic color of the oxide films varies with thickness in a well-understood manner,[21]

(20) Crank, J. *The Mathematics of Diffusion*; 2nd ed.; Oxford University Press: Oxford, UK, 1975.

(21) Anner, G. E. *Planar Processing Primer*; Van Nostrand Reinhold: New York, 1990.

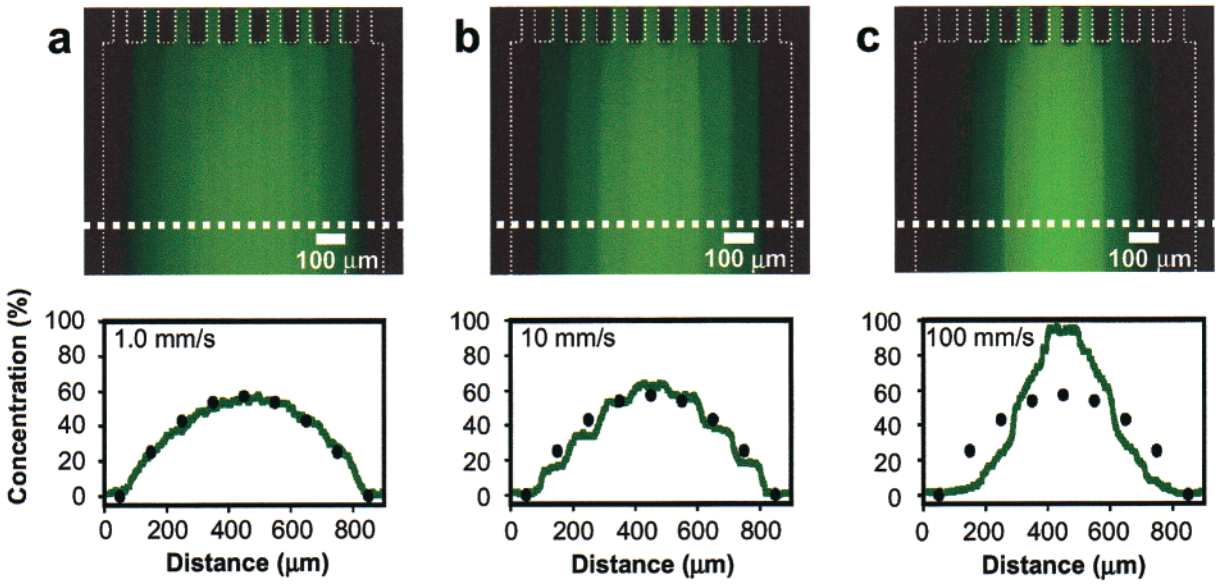

Figure 2. Fluorescence micrographs of solution gradient of FITC (fluorescein isothiocynate) at the outlet channel region shown at flow speeds of 1 mm/s (a), 10 mm/s (b), and 100 mm/s (c). A gradient generator similar in design to one described in Figure 1b was used. The plots below micrographs show the corresponding fluorescence intensity profile across the channel (900 μm wide) about 500 μm downstream (dotted line) from the junction. The calculated concentration of FITC in each branch channel is shown in round dots.

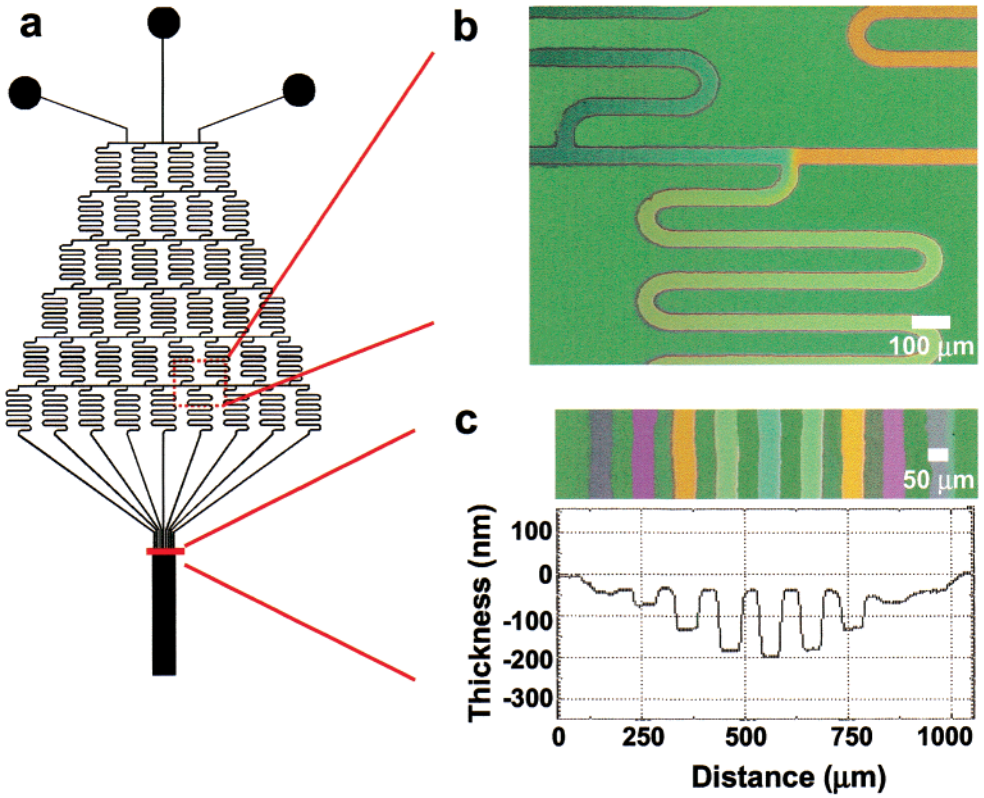

Figure 3. (a) Design of the microfluidic network used to generate a gradient in topography in SiO_2. Dilute HF (hydrofluoric acid, 5% in water) solution was introduced into the middle inlet and water into the two outer inlets. The microfluidic network generated a gradient in concentration of HF. Where the HF was in contact with the surface, it etched the SiO_2. The differences in the thickness of the SiO_2 layer gave rise to the different interference colors in the etched channels. (b) The top optical micrograph shows a junction where two streams containing different concentrations of HF were brought together. The color of the mixed channel was rapidly homogenized within a short distance from the junction (<500 μm) where the two fluid streams joined. (c) Optical micrograph and surface profilometer scan across the branch channels immediately before they are combined. The etched channel was deepest in the center channel, in agreement with the highest concentration of HF in that channel.

and is convenient for visualization of the gradient and (2) the depth of the etched SiO_2 layer measured with a surface profilometer can be compared with the value estimated from the color of the SiO_2 layer. Figure 3b shows the optical micrograph of a node where two streams containing different concentrations of HF are brought together. The different concentrations of HF that flowed through the channels are confirmed by the distinct color of the channels

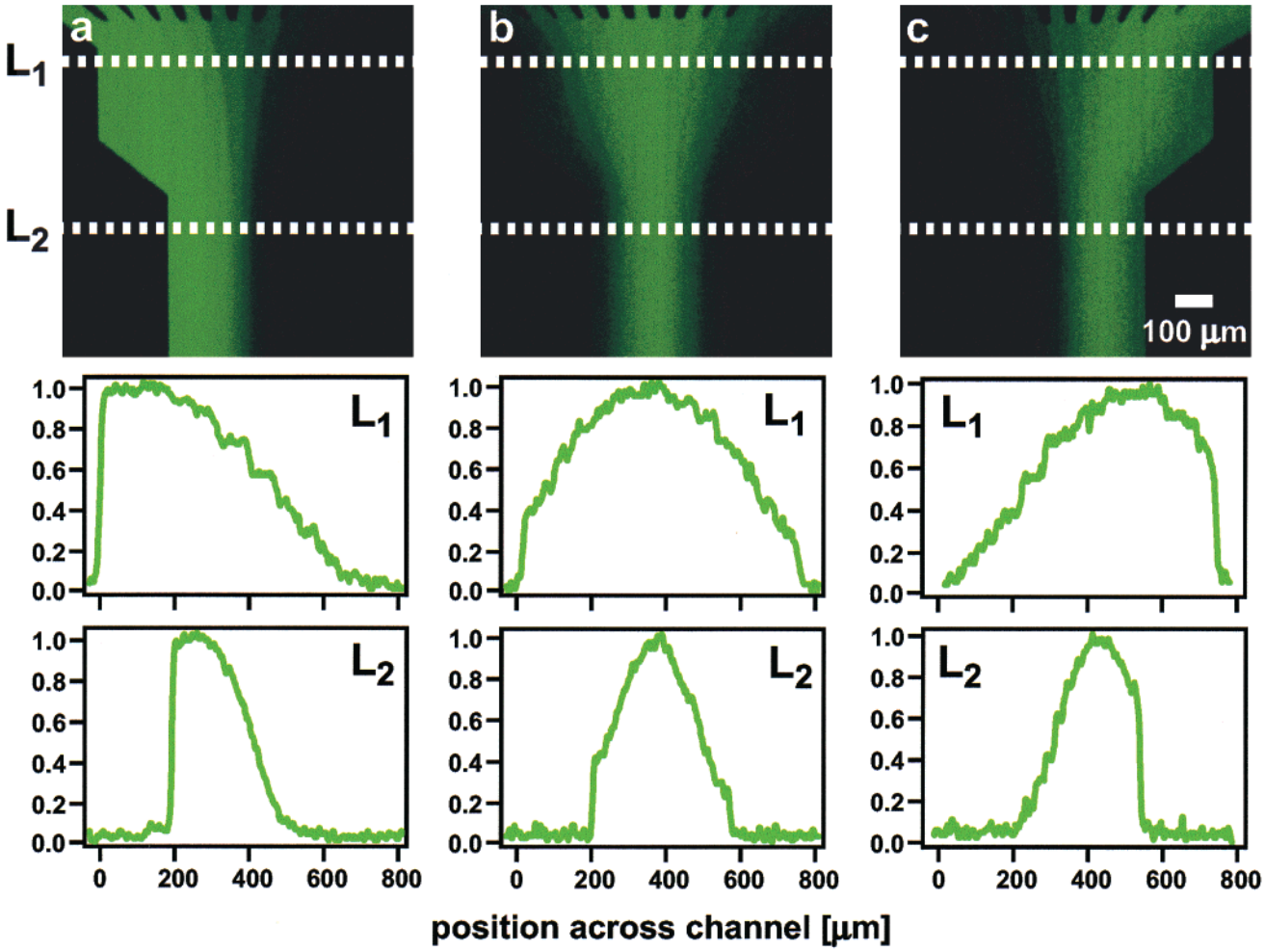

Figure 4. Fluorescence micrographs showing dynamic gradient of FITC that were obtained by varying the relative flow speed of the fluids at the inlets. The flow speed of the left inlet (buffer) was increased from (a) 0 mm/s, (b) 10 mm/s, and (c) 30 mm/s while holding the fluid speed of the other two inlets (FITC and buffer in middle and right inlets, respectively) constant at 10 mm/s. The peak of the concentration profile shifted from left to right as the fluid speed of left inlet was increased. The plots below micrographs show the corresponding fluorescence intensity profile across the channel 100 μm (L_1) and 500 μm (L_2) downstream (dotted lines) from the junction.

before and after they combine. The upper left channel (blue, ~310 nm thick SiO_2 on Si) contained higher concentration of HF than the upper right channel (orange, ~370 nm). The color of the channel becomes light green (340 nm) in the combined channel. This observation indicates that the diffusive mixing (following flow splitting described earlier) of relatively more concentrated flow (upper left channel) with the less concentrated flow (upper right channel) yielded a concentration that was between that of the two starting flows.

In addition, the color of the etched region changes from distinct blue and orange to uniform light green (~340 nm) within a short distance from the junction (<300 μm). This observation indicates fast, complete homogenization of HF concentration in the combined stream. Figure 3c shows the optical micrograph of the channels and the surface profilometer scan across them immediately before combining into a single large channel. The extent of etching in the channel was greatest at the center, in agreement with the calculation that the concentration of HF is highest in that part of the channel. The thickness of SiO_2 inferred from the color of the etched channels agrees well with the surface profilometer data. For example, the middle channel is 310 nm thick (blue, 310 nm = 500 − 190 nm, where 500 nm is the starting thickness and 190 nm is the depth of the etched center channel measured with the surface profilometer).

Dynamic Gradient. Figure 4 shows an example of a dynamic gradient that can be generated by varying the relative flow speeds of the inlet fluid flows. In this example, a pattern of channels similar to that used for Figure 3 with three inlets was used, but with a total of 15 branch channels. The channels were 50 μm wide and 100 μm high. It was possible to obtain dynamic gradients by changing the relative flow speed of the left inlet (buffer) while keeping the other two flow speeds constant at 10 mm/s (middle inlet = FITC, right inlet = buffer). Parts a, b, and c of Figure 4 correspond to flow speeds of 0, 10, and 30 mm/s for the left inlet. This figure shows that by changing the configuration of the experiment, a variety of gradients, both static and dynamic, can be created using a single type of gradient generator. In this case, by increasing the relative flow speed of the left inlet, the peak of the concentration profile was shifted from left to right.

The width of the gradient profile can be readily controlled over a range of values from 50 μm to several millimeters by changing the width of the final outlet channel. The resolution, which is calculated by dividing the width of the final outlet channel by the number of

branched channels, can be varied by changing the total number of branches that are combined into the outlet channel. It is thus straightforward to generate gradient profiles of various widths and resolutions (a larger number of branches yields higher resolution gradients) using the microfluidic approach. Figure 4 shows an example where the asymmetric concentration profile across 750 μm was reduced to 375 μm by simply changing the width of the outlet channel. Consequently, the width of each step in the gradient was effectively reduced from 50 μm to 25 μm.

Conclusions

The procedure described here provides a general method for generating gradients in chemical composition and surface topography using microfluidic systems molded in PDMS. The method is experimentally simple, highly adaptable, and requires no special equipment except for an elastomeric relief that can be readily prepared by rapid prototyping.[19,22,23] The design and fabrication of the gradient generator is simple: custom devices can be fabricated in less than 24 h using rapid prototyping and soft lithography. Although the application of these prototype devices, when fabricated in PDMS, is best suited for aqueous solutions, the method is general, and can be implemented in different solvent systems using appropriate materials (i.e., silicon, quartz, glass, and organic polymers) and fabrication methods.

There are a number of advantages in using microfluidic networks to generate gradients. First, a variety of gradients can be generated by using appropriate fluids or solutions (i.e., dye, etchants, solutions that form SAMs, and solutions of biomolecules such as proteins and small molecule drugs). These gradients, in principle, can be used to generate gradients in topology, medium, and surface, all in the same channel. Second, it is possible to generate gradients with resolution of several microns to several hundreds of microns (depending on the total number of branches and the width of the outlet channel where all the branches are combined); the larger channels are the right size to be relevant in studying cell biology (chemotaxis or haptotaxis). Third, gradients of different shapes (symmetric and asymmetric), types (smooth, step, and multiple peaks), and kinds (static and dynamic) can be obtained with modifications of the procedure, the microfluidic network design, or the implementation of the experiment (i.e. relative flow rates). Combining these systems with three-dimensional microfluidic networks[24,25] provides an additional level of control. Fourth, the microfluidic gradient generator can be used with a broad range of substrates.

In combination with the existing soft lithographic techniques that are used in patterning surfaces, cells, and biomaterials,[26,2726,27] the microfluidic gradient generator will provide a new tool for studying dynamic phenomena in cell biology and chemistry that depend on gradients in concentration. We believe that these methods will enable the generation of a range of solution and surface gradients and that they will be useful in studies of cell−surface interactions, chemotaxis, and haptotaxis.

Acknowledgment. This work was supported by DARPA and NSF (ECS-9729405). S.K.W.D. thanks the DFG (Deutsche Forschungsgemeinschaft) for a research fellowship. A.D.S. thanks the NIH for the Biophysics Training Grant (NIH GM30367).

LA000600B

(22) Qin, D.; Xia, Y.; Whitesides, G. M. *Adv. Mater.* **1996**, *8*, 917−919.

(23) Deng, T.; Tien, J.; Xu, B.; Whitesides, G. M. *Langmuir* **1999**, *15*, 5, 6575−6581.

(24) Anderson, J. R.; Chiu, D. T.; Jackman, R. J.; Cherniavskaya, O.; McDonald, J. C.; Wu, H.; Whitesides, S. H.; Whitesides, G. M. *Anal. Chem.* **2000**, *72*, 3158−3164.

(25) Jo, B. N.; VanLerberghe, L. M.; Motsegood, K. M.; Beebe, D. J. *J. Microelectromech. Syst.* **2000**, *9*, 76−81.

(26) Kane, R. S.; Takayama, S.; Ostuni, E.; Ingber, D. E.; Whitesides, G. M. *Biomaterials* **1999**, *20*, 2363−2376.

(27) Takayama, S.; Chapman, R. G.; Kane, R.; Whitesides, G. M. In *Application of Soft Lithography for Patterning of Cells and Their Environment*; Lanza, R., Ed.; Principles of Tissue Engineering, 2nd Edition; Academic Press: San Diego, 2000; pp 209−220.